JACS
JOURNAL OF THE AMERICAN CHEMICAL SOCIETY

Article

pubs.acs.org/JACS

Isomerizing Olefin Metathesis as a Strategy To Access Defined Distributions of Unsaturated Compounds from Fatty Acids

Dominik M. Ohlmann,[†] Nicole Tschauder,[‡] Jean-Pierre Stockis,[‡] Käthe Gooßen,[†] Markus Dierker,[§] and Lukas J. Gooßen*,[†]

[†]Fachbereich Chemie, Technische Universität Kaiserslautern, Erwin-Schrödinger-Straße 54, 67663 Kaiserslautern, Germany
[‡]Fachbereich Mathematik, Technische Universität Kaiserslautern, Erwin-Schrödinger-Straße 54, 67663 Kaiserslautern, Germany
[§]BASF Personal Care and Nutrition GmbH, Henkelstraße 67, 40551 Düsseldorf, Germany

Supporting Information

ABSTRACT: The dimeric palladium(I) complex $[Pd(\mu\text{-Br})\,{}^tBu_3P]_2$ was found to possess unique activity for the catalytic double-bond migration within unsaturated compounds. This isomerization catalyst is fully compatible with state-of-the-art olefin metathesis catalysts. In the presence of bifunctional catalyst systems consisting of $[Pd(\mu\text{-Br})\,{}^tBu_3P]_2$ and NHC−indylidene ruthenium complexes, unsaturated compounds are continuously converted into equilibrium mixtures of double-bond isomers, which concurrently undergo catalytic olefin metathesis. Using such highly active catalyst systems, the isomerizing olefin metathesis becomes an efficient way to access defined distributions of unsaturated compounds from olefinic substrates. Computational models were designed to predict the outcome of such reactions. The synthetic utility of isomerizing metatheses is demonstrated by various new applications. Thus, the isomerizing self-metathesis of oleic and other fatty acids and esters provides olefins along with unsaturated mono- and dicarboxylates in distributions with adjustable widths. The cross-metathesis of two olefins with different chain lengths leads to regular distributions with a mean chain length that depends on the chain length of both starting materials and their ratio. The cross-metathesis of oleic acid with ethylene serves to access olefin blends with mean chain lengths below 18 carbons, while its analogous reaction with hex-3-enedioic acid gives unsaturated dicarboxylic acids with adjustable mean chain lengths as major products. Overall, the concept of isomerizing metatheses promises to open up new synthetic opportunities for the incorporation of oleochemicals as renewable feedstocks into the chemical value chain.

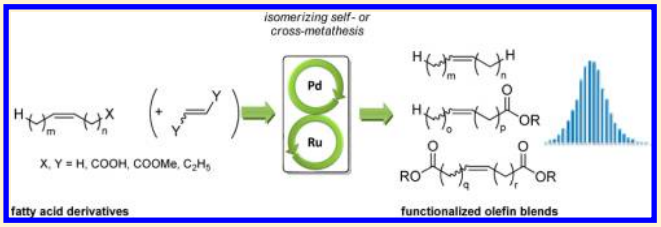

INTRODUCTION

Most of the present chemical value chain has evolved based primarily on petrochemical feedstocks. During steam cracking, crude oil is converted to olefin mixtures, which are then separated into fractions of similar chain lengths by distillation. Olefin blends with longer carbon chains are accessed on a hundred kiloton scale through the Shell Higher Olefin Process (SHOP), in which ethylene is converted into C_{10}−C_{18} olefins in a sequence of oligomerization, isomerization, and metathesis.[1] Due to their better availability, blends rather than single compounds are promising building blocks for polymers, surfactants, and plasticizers. The use of such defined mixtures of compounds with similar chain lengths potentially leads to better properties of the final bulk product than would be achievable for products derived from single compounds. For example, polymers resulting from mixed chain-length monomers would have reduced melting ranges and an improved processability, and detergents may display improved surface activity.

Due to the progressive depletion of crude oil, it is of high interest to increase the fraction of renewable feedstocks in the production of the above-mentioned commodities. In this context, plant oils are particularly attractive raw materials, because they provide long carbon chains (C16−C20) and are widely available on large scales. Current synthetic transformations include their ozonolysis, epoxidation, reduction, olefin metathesis, and enzymatic transformations.[2] Plant oil-derived products are already extensively used as surfactants, resins, lubricants, functionalized polymers, and coatings.[3]

A key factor that complicates a broader incorporation of fatty acids into the current chemical value chain is that only a few chain lengths are available from plant oils in sufficient abundance, oleic acid (**1b**) with its 18 carbon atoms being the most widely available. It can efficiently be functionalized at both its carboxylate group and its double bond, giving access to a variety of building blocks. The discovery of isomerizing functionalizations has further widened the spectrum of products accessible from this raw material. Isomerizing hydroformylations,[4] alkoxycarbonylations,[5] and hydroborations[6] allow its functionalization selectively in the ω-position. Five-membered ring lactones are obtained by isomerizing lactonizations,[7] while isomerizing 1,4-additions give rise to β-arylated and β-amino acids.[8]

Received: April 20, 2012
Published: July 20, 2012

   dx.doi.org/10.1021/ja303822c | J. Am. Chem. Soc. 2012, 134, 13716−13729

However, in all the above transformations, the entire aliphatic carbon backbone remains intact. It is not yet possible to convert oleic acid (**1b**) into compound mixtures with a chain-length distribution that is adjustable both with regard to its mean and span, in analogy to the olefin blends available from petrochemical sources.

We envisioned that isomerizing metatheses might present a solution to this challenge. If an effective catalyst system could be found that would continuously equilibrate the position of the double bond in olefinic substrates, such as oleic acid (**1b**), and at the same time continuously metathesize the olefin mixture, defined distributions of functionalized products should become available.

However, while the principal feasibility of isomerizing metatheses has been demonstrated (Scheme 1), substantial improvements in

Scheme 1. Pioneering Work in Isomerizing Self-Metatheses

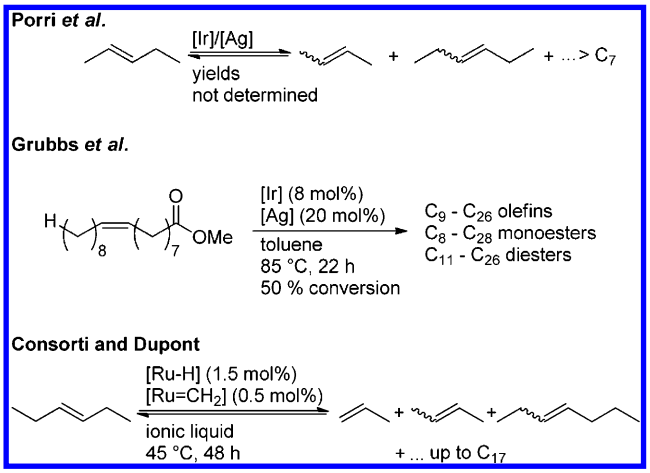

catalytic activity and functional group tolerance are needed before an application of this transformation to the valorization of **1b** becomes realistic. The first observation of a double-bond isomerization/cross-metathesis process dates back to 1975, when Porri et al. observed the formation of olefin mixtures rather than the expected polyolefins in the metathesis polymerization of olefins with iridium/silver systems.[9] Grubbs et al. demonstrated that the same catalyst can be used to convert 1-octadecene into an olefin mixture with a broad chain-length distribution.[10] Moreover, they showed that methyl oleate (**1a**) can be transformed into a mixture of olefins, unsaturated monoesters and α,ω-diesters, each with a range of chain lengths. However, despite high loadings of an expensive iridium/silver catalyst, the conversion remained incomplete, and the product distribution never reached its equilibrium state.

Recently, Consorti and Dupont have reevaluated the isomerizing metathesis of (*E*)-3-hexene (**9**) with a combination of 0.5 mol % modified Hoveyda–Grubbs metathesis catalyst and 1 mol % ruthenium hydride isomerization catalyst in an ionic liquid and obtained a mixture of olefins with up to 17 carbons.[11]

The valorization of fatty acids and esters, in particular, would benefit from isomerizing olefin metathesis processes.[10,11] Figure 1 illustrates the expected outcome of an isomerizing self-metathesis of oleic acid (**1b**) with an ideal catalyst system. In the course of the reaction, statistical mixtures of olefins, unsaturated monocarboxylates and dicarboxylates would form.

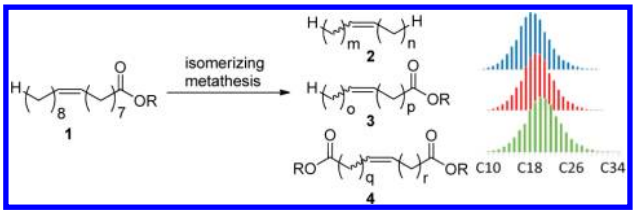

Figure 1. Expected product distribution in the isomerizing self-metathesis of oleic acid derivatives **1**.

The product fractions would cover a range of chain lengths, but the average chain length would remain at 18 carbon atoms.

Since the carbon chain lengths of the olefins would have to be equal at least to two, the unsaturated monocarboxylates to three, and the unsaturated dicarboxylates to four, the chain-length distributions of the three product classes would be slightly different from each other. With an ideal catalyst system, it should be possible to influence the widths of these distributions by stopping the reaction at various time points before complete conversion. When using bimetallic catalysts composed of one metal mediating the isomerization and the other the olefin metathesis, variation of their ratio would allow individually tuning the reaction rates and thus the composition of the product cuts.

The product and chain-length distributions obtained in isomerizing metatheses would also be affected by the addition of a second olefinic substrate such as ethylene or acrylic (**14b**) or maleic acid (**14c**). As in nonisomerizing metatheses, the selective removal of one of the products by evaporation or crystallization should allow shifting of the equilibrium toward one desired product class. The olefin fractions would be of interest as substitutes for intermediates otherwise obtained by the SHOP process, and the dicarboxylates, which are not easily accessible from petrochemical resources, should be useful precursors for novel bio-based polyesters, polyamides, and polyurethanes, as well as resins, fibers, coatings, and adhesives.[12]

However, several challenges needed to be overcome before such isomerizing metatheses could be achieved. The metathesis of **1b** itself is far from trivial, and only few catalysts are known to convert this substrate, which is available on scale only in moderate purity, contaminated with other fatty acids, terpenes, and further impurities. Moreover, both the isomerization and the metathesis catalysts would have to tolerate the presence of esters or even acidic carboxylate groups, and should have no detrimental effect on each other. This is hard to achieve because most known isomerization catalysts require activation with aggressive reagents such as metal hydrides, acids, or acid chlorides.[13] It is also likely that ligands would exchange between the two metal centers, resulting in the deactivation of both. Ru-based metathesis catalysts are well-known not to tolerate the presence of phosphine ligands. Another hurdle for the development of isomerizing metatheses of free fatty acids is that the latter tend to cyclize to the corresponding lactones in the presence of double-bond isomerization catalysts at elevated temperatures.[7] The entire process would thus have to be performed under very mild conditions and at low temperatures.

In the present work, we describe how these challenges were overcome with catalyst systems consisting of $[Pd(\mu\text{-}Br)^tBu_3P]_2$ as the isomerization catalyst and Hoveyda–Grubbs-type metathesis catalysts. They mediate the isomerizing self-metathesis of alkyl oleates and oleic acid (**1b**) at loadings below 1 mol %, as well as the isomerizing cross-metathesis with several short-chain olefins.

dx.doi.org/10.1021/ja303822c | J. Am. Chem. Soc. 2012, 134, 13716–13729

Table 1. Catalytic Double-Bond Isomerization of Methyl Oleate and Oleic Acid[a]

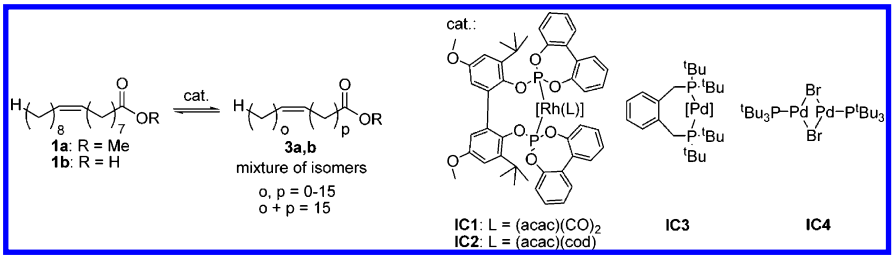

no.	R	catalyst (mol %)	solvent, T (°C)	result
1	Me	$PdCl_2$ (5)	EtOH, 80	double-bond shifted by up to 5 positions
2	Me	$RhCl_3 \cdot 3\ H_2O$ (2)	EtOH, 80	equilibrium distribution of double-bond isomers
3	Me	$Fe(CO)_5$ (20)	octane, 125	equilibrium distribution of double-bond isomers
4	Me	**IC1** (1.5)	toluene, 90	equilibrium distribution of double-bond isomers
5	Me	**IC2** (1.5)	toluene, 90	equilibrium distribution of double-bond isomers
6	Me	**IC3** (0.5)	neat, 70	no isomerization
7	Me	**IC4** (0.25)	neat, 70	equilibrium distribution of double-bond isomers
8	H	Rh(OTf)(cod) (1)	neat, 70	no isomerization
9	H	**IC1** (1.5)	toluene, 70	no isomerization
10	H	**IC2** (1.5)	toluene, 70	no isomerization
11	H	**IC3** (0.5)	neat, 70	double-bond shifted by up to 5 positions
12	H	**IC4** (0.25)	neat, 70	equilibrium distribution of double-bond isomers

[a]cod = 1,4-octadienyl. Reaction conditions: 0.5 mmol **1a** or **1b**, catalyst, solvent 1.0 mL (if appropriate), temperature given, 16 h, argon atmosphere. GC results after esterification with $MeOH/H_2SO_4$.

RESULTS AND DISCUSSION

Isomerization of Oleic Acid and Derivatives. The first step toward achieving an effective catalytic isomerizing metathesis was to identify an isomerization catalyst that would be active under the typical conditions of a double-bond metathesis. Oleic acid (**1b**) and its esters were expected to be more challenging substrates than simple olefins, so these were chosen as our initial model substrates.

In the context of our research on isomerizing functionalizations of fatty acids, we had extensively evaluated the activity of known isomerization catalysts.[8a] In continuation of these studies, we treated oleic acid (**1b**) with various known isomerization catalysts under literature conditions and investigated the progress of the isomerization by gas chromatography. Selected results are summarized in Table 1.

The results confirmed that few catalysts are capable of converting both methyl oleate (**1a**) and oleic acid (**1b**) into an equilibrium mixture of all 31 possible isomers, within less than 1 h, at below 1 mol % loading, and under neutral conditions. We considered this level of catalyst activity a prerequisite for the targeted process. Simple metal complexes were only found to promote the double-bond migration in **1a** and **1b** at high loadings and often required protic solvents (entries 1 to 3, 8). Solely rhodium bisphosphite complexes,[4,8a] such as **IC1** and **IC2**, displayed a high catalytic activity for the isomerization of methyl oleate (**1a**) even at low loadings (entries 4 to 5). Unfortunately, they did not promote the double-bond migration in oleic acid (**1b**) (entries 9 to 10). In contrast, palladium bisalkylphosphine complexes such as **IC3**[5] were active for the isomerization only of the acid but not of the ester (entry 11). According to the literature, such complexes require activation with strong acids,[5] which would, however, be incompatible with the metathesis catalyst.

Other catalysts described for isomerization processes were reported to be active only at higher temperatures.[14] They were neglected in this catalyst screening because of the thermal instability of metathesis catalysts, which precludes running the targeted isomerizing metathesis reactions above 70 °C. Another reason for avoiding high temperatures is the known cyclization of unsaturated carboxylic acids to the corresponding lactones in the presence of isomerization catalysts above 100 °C.[7a]

A control experiment revealed that the acidic conditions of the esterification do not lead to double-bond migration (see Supporting Information).

Since none of the established isomerization catalysts displayed the desired level of activity, we explored other metal complexes that we believed to have promising structural features that had not previously been described as isomerization catalysts.

The dimeric palladium complex $[Pd(\mu\text{-}Br)(^tBu_3P)]_2$ (**IC4**) caught our attention in this context. This complex was first reported by Mingos et al.[15] and has since been applied by Hartwig and others to various catalytic cross-coupling reactions, because of its pronounced ability toward aryl halide activation.[16] Although it had never been reported to display activity in double-bond isomerizations, we believed that it might be a good catalyst for this reaction because mechanistic studies have revealed that this unusual dimeric Pd(I) complex forms hydridopalladium(II) species under remarkably mild conditions. The addition of such Pd−H species across C−C double-bonds is believed to be the initiating step in olefin isomerization.[17]

The level of activity that **IC4** displayed in the isomerization of both oleic acid (**1b**) and methyl oleate (**1a**) surpassed all our expectations. A loading of only 0.25 mol % of this dimeric complex was sufficient to reach an equilibrium distribution of double-bond isomers for **1a** and **1b** within a few hours (entries 7 and 12, Table 1). Under these mild conditions, undesired side reactions, such as the formation of lactones[7] or of estolide oligomers,[18] were never observed.

The mechanism of the **IC4**-catalyzed isomerization could not yet be elucidated in full. In low-temperature NMR studies of the reaction solution in CD_2Cl_2, signals at −15.8 ppm

dx.doi.org/10.1021/ja303822c | J. Am. Chem. Soc. 2012, 134, 13716−13729

(t, $^2J_{H-P}$ = 6.9 Hz) were detected that likely pertain to monomeric palladium-hydride species.[19] Based on preliminary mechanistic studies and the work by Hartwig et al.,[20] we propose that the active catalyst is a $P^tBu_3Pd(H)Br$ species generated from the palladium dimer **IC4** along with a cyclometalated Pd(II)Br species.[21] We further assume that the catalytic cycle proceeds via the insertion of olefins into the Pd–H bond (Scheme 2).

Scheme 2. Postulated Mechanism of the Palladium-Catalyzed Double-Bond Migration

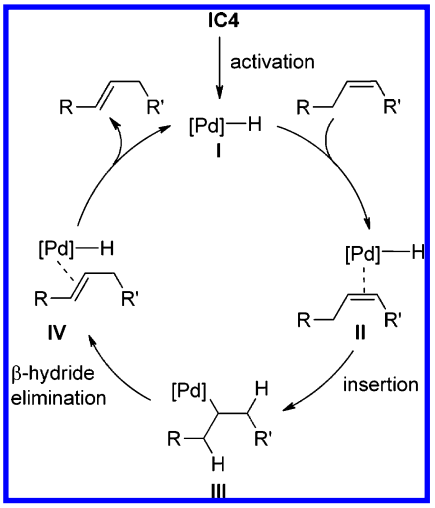

The great advantage of **IC4** as a catalyst precursor is that it bears only one phosphine per palladium. Release of phosphine ligands, which would inhibit the catalytic activity of the metathesis catalyst, is thus unlikely. Moreover, its activation does not require hydride or acid reagents, which could also be expected to have a negative impact on the metathesis catalyst.

With the discovery of this uniquely active isomerization catalyst, a decisive first milestone was reached en route to the desired isomerizing metathesis.

Self-Metathesis of Oleic Acid and Derivatives. The logical next step was to identify a suitable metathesis catalyst. We examined the catalytic activity of various ruthenium complexes for the self-metathesis of methyl oleate (**1a**) and oleic acid (**1b**), among them a Hoveyda–Grubbs first generation catalyst (**MC1**),[22] the Umicore-$M4_2$ (**MC2**)[23] and $M3_1$ catalysts (**MC3**),[24] a Hoveyda–Grubbs second generation catalyst (**MC4**),[25] Fürstner's catalyst (**MC5**),[26] the Umicore-$M1_1$ catalyst (**MC6**),[27] and the Umicore-$M4_1$ catalyst (**MC7**) (Figure 2).[23]

All of the depicted complexes displayed metathesis activity for methyl oleate (**1a**). However, only the catalysts Umicore-$M4_2$ (**MC2**) and Umicore-$M3_1$ (**MC3**) showed high catalytic activity also for the self-metathesis of oleic acid (**1b**) (Scheme 3).

The best results were achieved with **MC2**, which even at a 0.2% loading, led to 80% conversion of **1b** after 20 h at 45 °C in the absence of added solvent. This finding is in good agreement with reports by the groups of Dierker and Foglia.[28]

Isomerizing Self-Metathesis of Oleic Acid and Derivatives. With active catalysts in hand for both the isomerization and the metathesis reactions, we went on to evaluate their combination into a single process. The results obtained are summarized in Table 2.

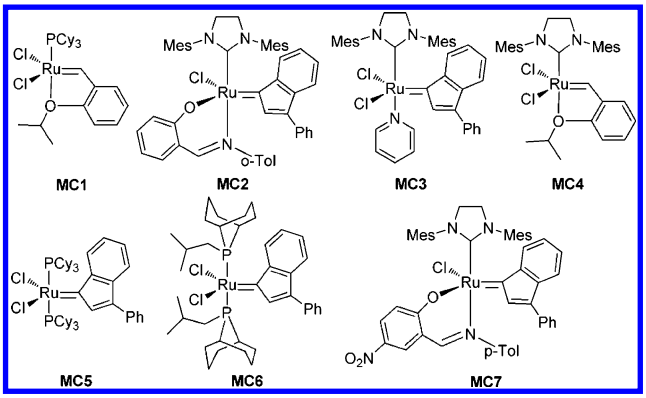

Figure 2. Metathesis catalysts investigated in this study.

Scheme 3. Self-Metathesis of Methyl Oleate and Oleic Acid

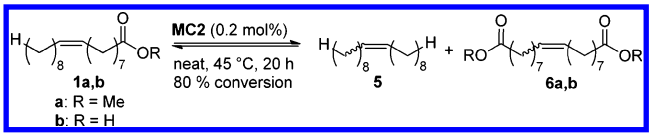

For methyl oleate (**1a**), the previously effective rhodium/bisphosphite complexes **IC1** and **IC2** turned out to be incompatible with the metathesis catalyst. Both lost their isomerization activity in the presence of the ruthenium complex. The metathesis reaction was also affected, leading to substantially reduced amounts of the self-metathesis products (entries 1 and 2). The palladium complex **IC3** showed no isomerization activity under neutral conditions but had a less detrimental effect on the metathesis catalyst, so that higher conversions were reached in the self-metathesis (entry 3).

In sharp contrast, the palladium dimer **IC4** retained its full isomerization activity and did not interfere with the metathesis of methyl oleate (**1a**). Within 20 h, **1a** was thus converted into an equilibrium mixture of olefins, monoesters, and diesters, each with a broad chain-length distribution (entry 4). Similar results were also obtained with catalyst **MC3** and the first generation Hoveyda–Grubbs catalyst **MC1** (entries 5 and 6). Fürstner's metathesis catalyst **MC5** completely shut down the isomerization activity of the palladium dimer **IC4**, which can be rationalized by the release of a phosphine during catalyst initiation, which then coordinates to the isomerization catalyst (entry 7). A similar observation was made for the Umicore-$M1_1$ catalyst (**MC6**).

In the isomerizing self-metathesis of oleic acid (**1b**) using the Umicore-$M4_2$ metathesis catalyst **MC2**, the rhodium/bisphosphite complexes **IC1** and **IC2** were unsuitable as cocatalysts, as anticipated from the isomerization studies above (entries 8 and 9). The palladium complex **IC3** and the metathesis catalyst **MC2** were reasonably compatible with each other, but the conversion remained incomplete (entry 10). Once again, the palladium dimer **IC4** performed best by far. In combination both with **MC2** and with **MC3**, full conversions of oleic acid (**1b**) were achieved (entries 11 and 12). Interestingly, the first generation Hoveyda–Grubbs catalyst **MC1** lost its catalytic activity in the presence of the palladium dimer **IC4** without negatively impacting the isomerization activity of the latter (entry 13). Since the other ruthenium catalysts had shown insufficient activity for the free acid even in the absence of an isomerization catalyst, they were not further considered in this study.

dx.doi.org/10.1021/ja303822c | J. Am. Chem. Soc. 2012, 134, 13716–13729

Table 2. Isomerizing Self-Metathesis of Methyl Oleate and Oleic Acid[a]

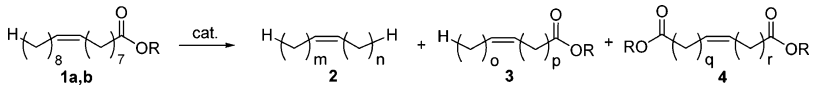

no.	R	met. cat.	isom. cat.	conv. (%)	comments
1	Me	**MC2**	**IC1**	10	no isomerization, ca. 10% self-metathesis products
2	Me	**MC2**	**IC2**	50	no isomerization, ca. 50% self-metathesis products
3	Me	**MC2**	**IC3**	70	no isomerization, ca. 65% self-metathesis products
4	Me	**MC2**	**IC4**	full	isomerizing self-metathesis close to equilibrium
5	Me	**MC3**	**IC4**	full	isomerizing self-metathesis close to equilibrium
6	Me	**MC1**	**IC4**	full	isomerizing self-metathesis close to equilibrium
7	Me	**MC5**	**IC4**	50	<20% isomerizing self-metathesis, ca. 40% self-metathesis products
8	H	**MC2**	**IC1**	55	<10% isomerizing self-metathesis, ca. 40% self-metathesis products
9	H	**MC2**	**IC2**	<5	no isomerization, traces of self-metathesis products
10	H	**MC2**	**IC3**	55	<10% isomerizing self-metathesis, ca. 40% self-metathesis products
11	H	**MC2**	**IC4**	full	isomerizing self-metathesis close to equilibrium
12	H	**MC3**	**IC4**	full	isomerizing self-metathesis close to equilibrium
13	H	**MC1**	**IC4**	full	isomerization into equilibrium distribution, no self-metathesis products

[a]Reaction conditions: 3.0 mmol of substrate **1a** or **1b** (90% purity), 0.5 mol % isomerization catalyst, 0.2 mol % metathesis catalyst, neat, 45 °C for Rh catalyzed reactions or 70 °C for Pd catalyzed reactions, 20 h, argon atmosphere. The reaction mixtures were analyzed by GC after esterification with H_2SO_4/MeOH.

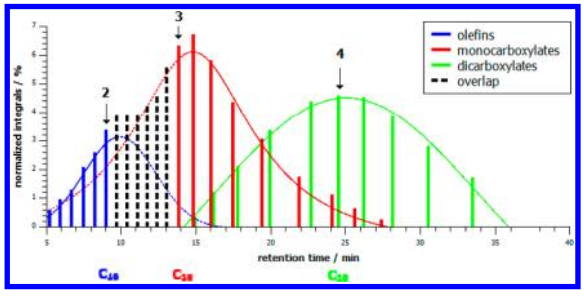

Figure 3. Product distributions obtained in the isomerizing self-metathesis of oleic acid (**1b**). Reaction conditions: 1.0 mmol of **1b**, 0.6 mol % **IC4**, 0.5 mol % **MC2**, hexane 3.0 mL, 70 °C, 20 h, argon atmosphere. GC results after esterification with MeOH/H_2SO_4.

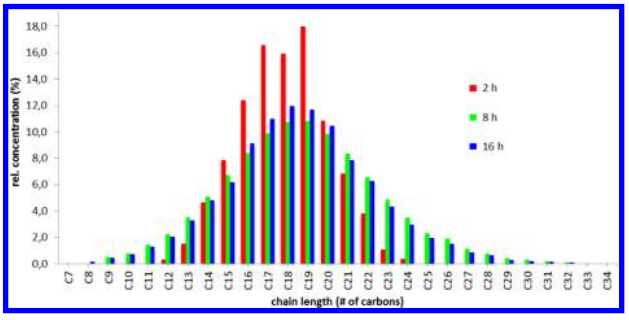

Figure 4. Reaction progress of the isomerizing self-metathesis of oleic acid (**1b**) visualized through the olefin chain-length distribution. Reaction conditions: 0.5 mmol of **1b**, 0.6 mol % **IC4**, 0.5 mol % **MC2**, 2.0 mL of hexane, 60 °C, argon atmosphere.

The results of the isomerizing self-metathesis of **1b** in the presence of 0.5 mol % **MC2** and 0.6 mol % palladium dimer **IC4** in hexane are visualized in Figure 3. The individual gas-chromatographic signals were assigned to olefins, monocarboxylates, and dicarboxylates based on mass spectral data. Since the peak shapes vary strongly for the product classes, a histogram was generated in which the integrals of the GC peaks are plotted against the retention times. Idealized curves were superimposed on this processed GC to visualize the distributions for each product class. When interpreting the plots, one must take into account that the areas below these curves do not represent the relative occurrence of each product class, because the signal spacing increases from left to right and because the individual integrals are uncorrected for response factors.

Uniform, broad chain-length distributions for all product fractions were obtained under the conditions described above. The chain-length distribution of the olefin fraction reaches up to at least C_{26}. Unsaturated monocarboxylates were detected from C_{13} to C_{25}, dicarboxylates from C_{13} to C_{22}.

The progress of the isomerizing self-metathesis of oleic acid (**1b**) was monitored over time to confirm that the product distribution indeed reached its maximum width under these conditions. To simplify product analysis and maximize the detection sensitivity, the unfunctionalized olefin fraction was selectively extracted from the reaction mixture and analyzed by GC/GC-MS. The histograms in Figure 4 reveal that after 2 h at 60 °C, the product distribution is still relatively sharp. It continuously broadens over the subsequent 6 h, but is not further impacted beyond that point in time. This confirms that after 8 h, an equilibrium composed mainly of olefins ranging from C_8 to C_{32} is reached.

We next probed whether the product distribution of the isomerizing self-metathesis can be tuned by adjusting the reaction conditions. Upon reduction of the reaction temperature to 25 °C under otherwise identical conditions, double-bond migration is completely shut down, while the olefin metathesis still reaches its equilibrium. Thus, in the presence of 0.6 mol % **IC4** and 0.5 mol % **MC2** at 25 °C in hexane, a 1:1:1 mixture of oleic acid (**1b**), 1,18-octadec-9-enedioic acid (**3b**), and 9-octadecene (**4**) is formed. The observed influence of the reaction temperature on the rate of the isomerization but not on the metathesis should allow tuning the width of the product distribution simply by choosing the appropriate temperature within a range of 25 to 70 °C.

At 40 °C, equal amounts of olefins and mono- and dicarboxylates were indeed formed, each with a very narrow

dx.doi.org/10.1021/ja303822c | J. Am. Chem. Soc. 2012, 134, 13716−13729

chain-length distribution around the C_{18} self-metathesis products **1**, **5**, and **6** (Figure 5).

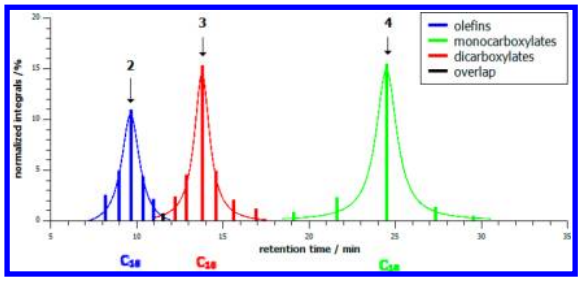

Figure 5. Product distribution resulting from the isomerizing self-metathesis of oleic acid (**1b**). Reaction conditions: 1.00 mmol of **1b**, 0.6 mol % **IC4**, 0.5 mol % **MC2**, hexane 3.0 mL, 40 °C, 20 h, argon atmosphere.

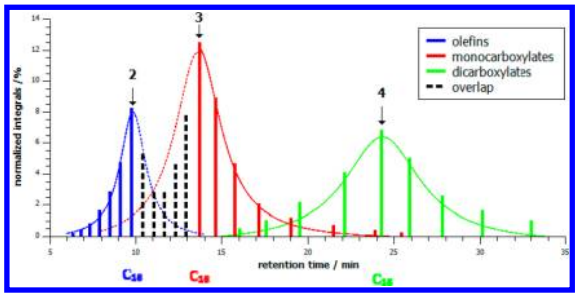

Figure 6. Product distribution resulting from the isomerizing self-metathesis of oleic acid (**1b**). Reaction conditions: 1.0 mmol of **1b**, 1.2 mol % **IC4**, 0.5 mol % **MC2**, neat, 60 °C, 8 h, argon atmosphere.

The isomerizing metathesis of oleic acid (**1b**) can also be performed under solvent-free conditions. Since this somewhat reduces the activity of the isomerization catalyst, its loading needs to be increased to 1.2 mol %. Figure 6 visualizes the outcome of an isomerizing self-metathesis of neat oleic acid (**1b**). The reaction mixture was stirred for 8 h using 1.2 mol % of **IC4** and 0.5 mol % of **MC2** as the catalyst system. After this short reaction time, the product distributions are still relatively narrow and consist of C_{12}–C_{24}-olefins, C_{12}–C_{25}-monocarboxylates, and C_{14}–C_{22}-dicarboxylates.

The metathesis catalyst **MC3** combined with **IC4** promotes the isomerizing self-metathesis of **1b** at lower temperatures than **MC2**. Even after reducing the **IC4**-loading to 0.3 mol %, full equilibrium was still reached using 0.5 mol % **MC3** at 50 °C in hexane (Figure 7, see Figure 3 for comparison).

In order to reach fully equilibrated product distributions as in Figures 3 and 7, both the isomerization and metathesis catalysts must react with each double bond in the reaction mixture not only once but several times. Turnover numbers (TON) calculated using the conversion of the olefin starting material are thus not very meaningful to map out the reaction progress. Still, a rough impression of the high efficiency of the catalyst system may be obtained when one considers that for combinations of 0.01 mol % **IC4** and 0.025 mol % of either **MC2** or **MC3**, more than 50% of the products have chain lengths other than 18, corresponding to a TON > 2000 for both the isomerization and the olefin metathesis.

Isomerizing Self-Metathesis of Other Fatty Acids. With a catalyst system consisting of 0.5 mol % **IC4** and 0.6 mol % **MC2**, other fatty acids beside oleic acid derivatives were

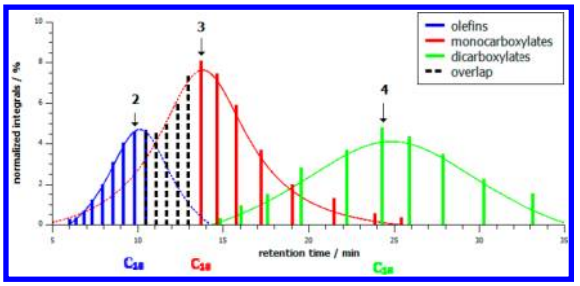

Figure 7. Product distribution resulting from the isomerizing self-metathesis of oleic acid (**1b**). Reaction conditions: 1.0 mmol of **1b**, 0.3 mol % **IC4**, 0.5 mol % **MC3**, hexane 3.0 mL, 50 °C, 20 h, argon atmosphere.

Scheme 4. Isomerizing Self-Metathesis of 10-Undecenoic and Linoleic Acids

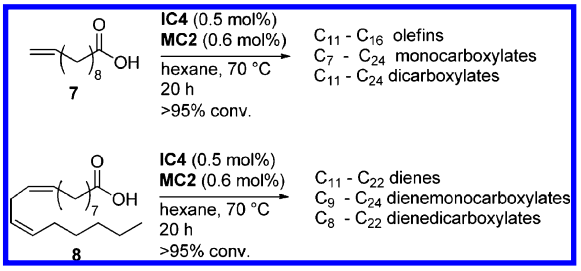

successfully converted, among them 10-undecenoic acid (**7**) and linoleic acid (**8**, Scheme 4).

Compound **7** is a particularly interesting example since at the outset, the double bond is in the terminal position. Thus, the product distribution initially has additional maxima for long- and short-chain products. However, due to the high efficiency of the isomerization catalyst, it converges toward the usual equilibrium distributions for all three product classes within 20 h, even at low catalyst loadings.

Linoleic acid (**8**) is another challenging substrate, as it contains two double-bonds that may be moved into conjugation. Although conjugated dienes are known to interfere with transition metal-based isomerization catalysts,[29] the standard conditions still led to full conversion of this substrate.

Isomerizing Metathesis of Simple Olefins. The performance of the new bimetallic catalyst system was benchmarked also for simple olefins such as (*E*)-3-hexene (**9**). Consorti and Dupont had found that the isomerizing olefin metathesis of this substrate requires 2 days using 0.5 mol % of a ruthenium-hydride isomerization catalyst and 1 mol % of a modified Hoveyda–Grubbs metathesis catalyst in an ionic liquid solvent.[11] Our catalyst system promoted this reaction with substantially higher efficiency. Already at loadings of 0.1 mol % of the palladium dimer **IC4** and 0.2 mol % of the second generation Hoveyda–Grubbs catalyst **MC4**, the reaction reached its equilibrium within only 16 h (Scheme 5).

Scheme 5. Isomerizing Self-Metathesis of (*E*)-3-Hexene

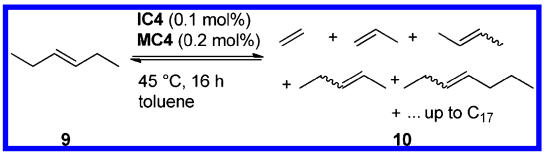

dx.doi.org/10.1021/ja303822c | J. Am. Chem. Soc. 2012, 134, 13716–13729

The resulting olefin mixture shows the expected chain-length distribution with a maximum at C_6 and a shallow downward slope toward higher olefins (Figure 8, red bars). Chains with

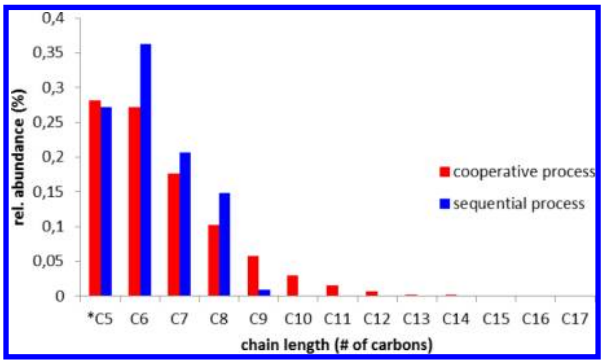

Figure 8. Chain-length distribution obtained in the cooperative isomerizing self-metathesis of **9** (red) and in the analogous sequential process (blue). *C_5 fraction may contain unresolved C_4 and C_3 olefins.

more than 17 carbon atoms were detectable in trace quantities. In contrast, chains with only up to 10 carbon atoms are accessible via a consecutive isomerization and metathesis of (*E*)-3-hexene (**9**, Figure 8, blue bars).

Beyond the isomerizing self-metathesis of olefins, in which the mean chain length always remains unchanged, one could imagine related processes in which not only the distribution shapes but also the mean chain lengths of the olefin mixtures are tunable. Thus, the isomerizing cross-metathesis of a mixture of two olefins with different chain lengths should, in principle, allow the synthesis of olefin blends with mean chain lengths ranging anywhere between the lengths of the two starting materials. Adjustment of the mean chain length should be possible simply by changing the ratio between the two starting materials. This concept is illustrated in Scheme 6 using

Scheme 6. Isomerizing Cross-Metathesis of (*E*)-3-Hexene and 1-Octadecene

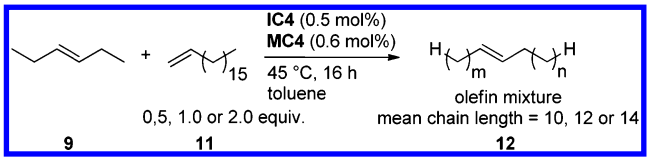

the example of an isomerizing cross-metathesis of 1-octadecene (**11**), available from oleochemical sources, with a short-chain olefin.

Indeed, the isomerizing metathesis of a 1:1 mixture of 1-octadecene (**11**) with (*E*)-3-hexene (**9**) in the presence of 0.6 mol % Pd-dimer **IC4** and 0.5 mol % metathesis catalyst **MC4** led to a uniform product distribution with the expected mean chain length of 12 carbon atoms. The use of a long-chain olefin unsaturated at the terminal position poses a particular challenge for the isomerization catalyst. During the first hours of the reaction, an irregular distribution with local maxima at chain lengths of 34 and 6 carbon atoms were observed. However, after 20 h, an almost ideal distribution was reached, further demonstrating the high activity of the catalyst system (Figure 9, red bars).

Figure 9 also illustrates the fundamental difference between an isomerizing olefin metathesis on one hand, and a sequential process of double-bond isomerization followed by metathesis

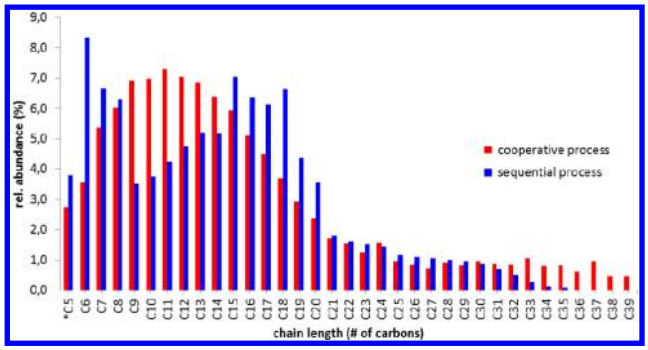

Figure 9. Cooperative (red) and sequential (blue) processes for the isomerizing cross-metathesis of (*E*)-3-hexene (**9**) and 1-octadecene (**11**). *C_5 fraction may contain unresolved C_4 and C_3 olefins.

on the other. For the sequential reaction, both olefins were initially converted into an equilibrium mixture of positional isomers by reaction with the isomerization catalyst **IC4**. The catalyst was then separated from the olefin mixture by filtration through basic alumina. Subsequently, the olefin mixture was allowed to react in the presence of the metathesis catalyst **MC4**. The sequential process leads to an entirely different chain-length distribution, with maxima around C_6, the initial chain length of the hexene, and C_{18}, the most likely chain length of a self-metathesis product of octadecene (Figure 9, blue bars).

This experiment confirmed that cooperative action of the isomerization and metathesis catalysts leads to a smooth chain-length distribution even under challenging conditions. Such product mixtures not only are useful as monomers but also can be functionalized further, for example, via isomerizing alkoxycarbonylations, hydroborations, or hydroformylations.[4−6] The overall processes would open up additional opportunities for the incorporation of carbon atoms derived from oleochemical sources into the chemical value chain.

We next probed whether the mean chain length can indeed be controlled by varying the ratio of olefin starting materials. We thus mixed (*E*)-3-hexene (**9**) with 1-octadecene (**11**) in three different ratios and subjected them to isomerizing olefin metathesis using 0.5 mol % **IC4** and 0.6 mol % **MC4** as the catalyst system (see Scheme 6). Regular chain-length distributions were obtained in all cases (Figure 10). The

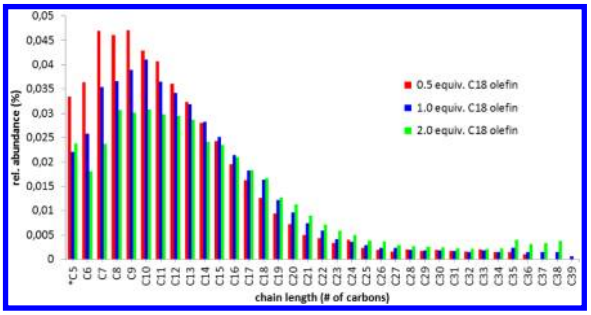

Figure 10. Product distributions resulting from cross-metathesis of **9** and **11** with different ratios. *C_5 fraction may contain unresolved C_4 and C_3 olefins.

maxima of the distributions reflect the expected shift in the mean chain length resulting from changing the ratio of the two starting materials. With 0.5 equiv of 1-octadecene (**11**), the calculated mean is C_{10} (red bars), with 1 equiv of **11** it is C_{12} (blue bars), and with 2 equiv of **11** it is C_{14} (green bars).

dx.doi.org/10.1021/ja303822c | J. Am. Chem. Soc. 2012, 134, 13716−13729

Mathematical Prediction of the Product Distributions. The overall trends in the product distributions are clearly visible from the experimental data. However, there are several factors that may cause experimental deviations from the theoretical reaction outcome. One has to take into account that short-chain olefins with chain lengths below C_5 partially evaporate during the reactions, resulting in a shift of the detected chain-length distribution toward longer chains. Due to their volatility, these olefins are not detected quantitatively in the gas chromatograms, preventing an exact quantification of the product fractions. Moreover, the GC response factors can be expected to vary slightly for each olefin. Because of these analytical issues, it was desirable to develop a method to calculate ideal product distributions for isomerizing metatheses.

In order to predict equilibrium distributions of the product fractions, we designed a mathematical simulation of the reaction using the statistics software R.[30] The following base assumptions were made: (1) All reaction products remain in the reaction solution; (2) all double-bond isomers have the same stability, which means that the double-bond will be in any position of the carbon chain with the same probability; (3) the isomerization proceeds substantially faster than the metathesis, so that full equilibration of the double-bond position occurs between each metathesis step. For the calculations discussed below, the program was parametrized such that the metathesis proceeds with a similar reaction rate for each double-bond isomer.

The program is based on a Markov process using a modified sample-with-replacement method to simulate the progress of the chemical reaction. The situation at the onset of the reaction is described by a vector containing the chain length of all individual molecules that are available for reaction with a single molecule of the metathesis catalyst. In the first step, the initiation of the metathesis catalyst molecule is simulated by randomly selecting one olefin molecule, cleaving it at a random position and attaching one part to the metathesis catalyst. In each subsequent step, this residue is combined with one part of another randomly selected olefin, while the other part of the olefin remains at the catalyst. The vector of olefin molecules is then updated, and the process is repeated until the desired number of iterations is reached.

Using this simulation program, the chain-length distributions were predicted for isomerizing metatheses of 200 olefin molecules, which corresponds to isomerizing metatheses using 0.5 mol % metathesis catalyst. Fluctuation of the results can be reduced to a more realistic degree when averaging 100 runs. This roughly approximates an experimental situation in which 100 catalyst molecules react with 20 000 olefin molecules. In the chemical experiments, 10^{18} catalyst molecules convert 10^{20} olefin molecules, which reduces fluctuation to a negligible amount.

We first investigated how many turnovers of the metathesis catalyst are required to fully convert the olefin starting materials and to achieve the experimentally observed regular distributions. This was performed using dodecene (Figure 11).

Using up to 1000 steps, which correspond to an average of five metathesis steps per molecule, an overproportional amount of C_{12} molecules is still seen in the simulation. The distribution shape is a result of the parametrization of the program, in which the double-bond migration is simulated to be substantially faster than the olefin metathesis. Thus, at incomplete conversion, left-over C_{12} starting material isomers along with products spanning the full width of the equilibrium distribution

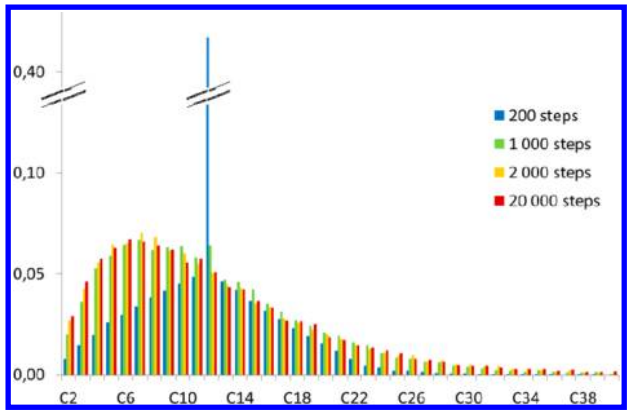

Figure 11. Calculated distributions for the self-metathesis of dodecene.

are observed, rather than narrow distributions that gradually broaden (see Figure 5). The simulation gets sufficiently close to the equilibrium distribution at a TON of 2000 or above (on average 10 metathesis steps per olefin molecule). These calculations demonstrate that the TONs for the metathesis catalyst are at least 10 times higher than the substrate-to-catalyst ratio would suggest (see the discussion of experimental TONs, above).

Figure 12 depicts the overlaid histograms calculated for 200 dodecene molecules versus 100 hexene and 100 octadecene

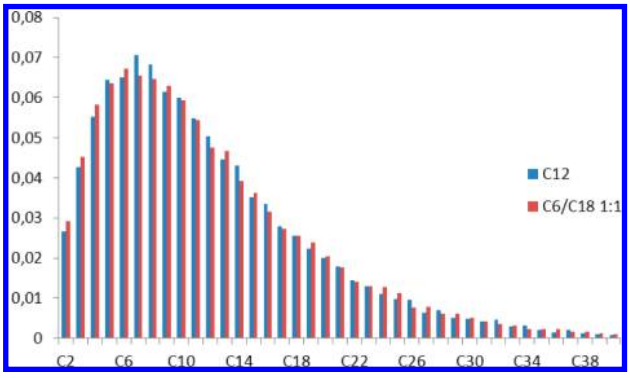

Figure 12. Calculated distributions for the metatheses of dodecene and a 1:1 octadecene/hexene mixture.

molecules; each as an average of 100 runs with 2000 steps. Their congruence demonstrates that after each molecule has been metathesized on average ten or more times, the reaction outcome of isomerizing metatheses is dependent only on the mean chain length and not on the starting material composition. This corresponds well with the experimental observations discussed below Scheme 6.

Figure 13 shows superimposed histograms corresponding to simulations with 200 olefins with 3, 6, and 12 carbons, each as an average over 100 runs, to demonstrate the influence of the mean chain length on the shape of the product distribution. The shapes of the histograms change from being exponential-like (C_3) to being Boltzmann-like with sharp (C_6) and finally broad maxima (C_{12}) (Figure 13). These shapes are as expected for an array of molecules with a defined mean, a defined left-hand chain length limit at C_2, and a right-hand chain length that is unlimited.

Overall, the simulation program allows prediction of the experimental outcomes of isomerizing metatheses based on the

dx.doi.org/10.1021/ja303822c | J. Am. Chem. Soc. 2012, 134, 13716−13729

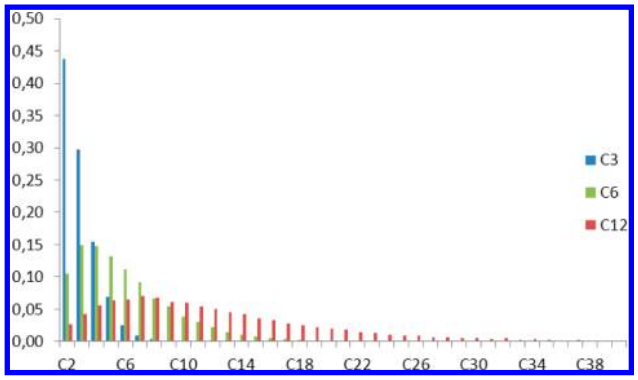

Figure 13. Calculated distributions for the metatheses of propene, hexene, and dodecene.

mean carbon-chain length of the olefin starting materials. It represents an important first step toward finding an analytical formula to describe the relative abundance of each carbon chain based only on the mean chain length. This is the subject of ongoing research.

Isomerizing Ethenolysis of Fatty Acids. In continuation of the experimental studies, we next evaluated whether it is also possible to adjust the chain lengths of fatty acid-derived products by adding defined amounts of a cross-metathesis partner. Thus, the use of a suitable metathesis catalyst and an ethylene atmosphere would allow incorporation of this C_2-building block into the product fractions obtained by isomerizing cross-metathesis of oleic acid derivatives. This would result in a considerable shift of the mean chain length toward lower carbon-chain lengths. At the same time, the ratio of olefins and mono- and dicarboxylates will shift toward the olefin fraction because of the additional unfunctionalized chain ends.

In order to make this cross-metathesis work, the metathesis catalyst needed to activate ethylene and oleic acid derivatives at comparable rates. We searched for a suitable bimetallic catalyst system using the isomerizing ethenolysis of methyl oleate (**1a**) and oleic acid (**1b**), starting from the reaction conditions optimized for their isomerizing self-metathesis (Table 3). Neither **MC2** nor **MC1** displayed any activity for the cross-metathesis of **1a** or **1b** with ethylene (entries 1, 2, 6, and 7). Moreover, in their presence and under an ethylene atmosphere, **IC4** appeared to lose its isomerization activity (entries 1, 2, 6, and 7). In contrast, both the **MC3**/**IC4** and the **MC7**/**IC4** combinations remained active in the presence of ethylene (entries 3–5, 8). With a catalyst system consisting of 0.6 mol % **MC3** and 0.6 mol % **IC4**, 85% conversion was reached in the isomerizing ethenolysis of methyl oleate (**1a**) (entry 4). Similarly, a catalyst system consisting of 0.6 mol % **MC7** and 0.5 mol % **IC4** led to full conversion in the isomerizing ethenolysis of oleic acid (**1b**) (entry 8).

Further investigations revealed that the desired regular product distribution with a single maximum, indicative of full equilibration, could be reached with loadings above 1.5 mol % of the metathesis catalyst and 0.75 mol % of the isomerization catalyst (entries 9 to 12). Any additional increase in the loadings of both catalysts no longer influenced the shape of the product distribution. This is illustrated in Figure 14, which shows histograms of the olefin product fractions obtained by hexane extraction of the basified reaction mixtures. The mono- and diacids displayed similar distribution patterns.

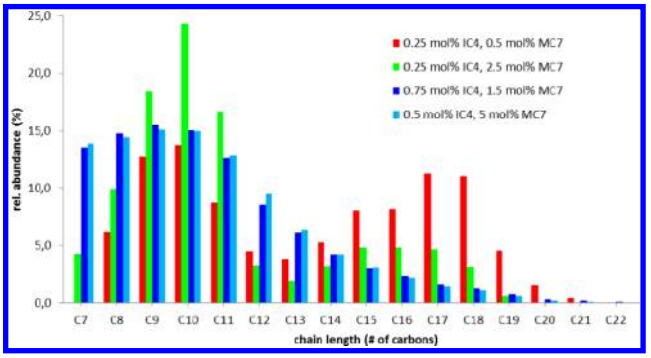

Figure 14. Chain-length distributions of the olefin fraction from the isomerizing ethenolysis of oleic acid (**1b**).

Table 3. Optimization of the Isomerizing Ethenolysis of Oleic Acid Derivatives[a]

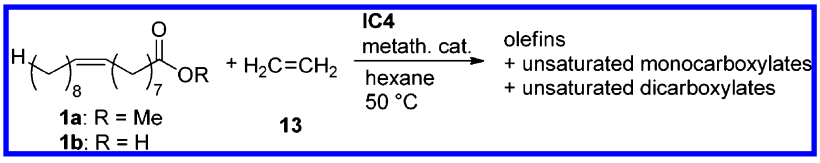

no.	**IC4** (mol %)	metath. cat. (mol %)	R	conv.[b] (%)	comment
1	0.5	**MC2** (0.6)	Me	35	no isomerization, ca. 20% self-metathesis, ca. 15% ethenolysis
2	0.5	**MC1** (0.6)	Me	<5	
3	0.5	**MC7** (0.6)	Me	59	ca. 25% nonisomerizing self-metathesis, ethenolysis detectable
4	0.5	**MC3** (0.6)	Me	85	isomerizing ethenolysis, distribution is far from equilibrium
5	0.5	**MC3**(0.6)	H	65	isomerizing ethenolysis, distribution is far from equilibrium
6	0.5	**MC2**(0.6)	H	60	no isomerization, 54% self-metathesis, no ethenolysis
7	0.5	**MC1** (0.6)	H	<5	
8	0.5	**MC7** (0.6)	H	full	isomerizing ethenolysis, distribution is far from equilibrium
9	0.25	**MC7** (0.5)	H	full	isomerizing ethenolysis, distribution is far from equilibrium
10	0.75	**MC7** (1.5)	H	full	isomerizing ethenolysis, distribution is close to equilibrium
11	0.25	**MC7** (2.5)	H	full	isomerizing ethenolysis, distribution is far from equilibrium
12	0.5	**MC7** (5.0)	H	full	isomerizing ethenolysis, distribution is close to equilibrium

[a]Reaction conditions: 0.5–1.0 mmol of substrate **1a** or **1b**, isomerization catalyst **IC4**, metathesis catalyst, 6.0 mL of hexane/mmol substrate, 50 °C, ethylene atmosphere, 16 h. [b]Conversion of the substrate **1a** or **1b**, analysis of the product mixtures by GC after esterification with $MeOH/H_2SO_4$.

dx.doi.org/10.1021/ja303822c | J. Am. Chem. Soc. 2012, 134, 13716–13729

Table 4. Optimization of the Isomerizing Cross-Metathesis of 1a and 1b with Different Olefins[a]

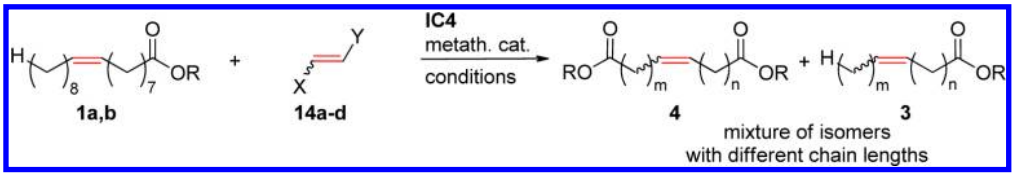

no.	R	X, Y	IC4 (mol %)	metath. cat. (mol %)	solvent	conv. (%)[b]	comment
1	Me	H, COOMe	1	**MC2** (1.5)	neat	25	predominantly self-metathesis, no cross-metathesis products
2	Me	H, COOH	1	**MC2** (1.5)	neat	20	predominantly self-metathesis, no cross-metathesis products
3	H	H, COOMe	1	**MC2** (1.5)	neat	31	predominantly self-metathesis, no cross-metathesis products
4	H	H, COOH	1	**MC2** (1.5)	neat	39	predominantly self-metathesis, no cross-metathesis products
5	H	COOH, (*Z*)-COOH	0.75	**MC2** (1.5)	neat	80	isomerizing self-metathesis, no cross-metathesis products
6	H	COOH, (*Z*)-COOH	0.75	**MC2** (1.5)	hexane	85	isomerizing self-metathesis, no cross-metathesis products
7	Me	COOH, (*Z*)-COOH	2.5	**MC2** (1.5)	THF	full	isomerizing cross-metathesis far from equilibrium, no shift of mean chain length
8	Me	COOH, (*Z*)-COOH	2.5	**MC2** (1.5)	toluene	full	isomerizing cross-metathesis far from equilibrium, no shift of mean chain length
9	H	CH_2COOH, (*E*)-CH_2COOH	2.5	**MC7** (5.0)	THF	full	isomerizing cross-metathesis close to equilibrium, significant shift of mean chain length

[a]Reaction conditions: 0.25 mmol of substrate **1a** or **1b**, 0.25−1.25 mmol of coupling partner **14a−d**, isomerization catalyst **IC4**, metathesis catalyst, 1.5 mL of solvent, if appropriate, 70 °C, 16 h, argon atmosphere. [b]Conversion of the substrate **1a** or **1b**, analysis of the product mixtures by GC after esterification with $MeOH/H_2SO_4$.

Isomerizing Cross-Metathesis of Fatty Acids with Dicarboxylic Acids. The isomerizing cross-metathesis of oleic acid (**1b**) with a short-chain unsaturated mono- or dicarboxylic acid should lead to the formation of predominantly mono- or dicarboxylic acids with medium chain lengths. To probe the feasibility of this approach, we investigated various carboxylate-containing substrates in isomerizing cross-metatheses with oleic acid (**1b**) or methyl oleate (**1a**). As can be seen in Table 4, neither acrylic acid (**14b**) nor methyl acrylate (**14a**) gave satisfactory results with a catalyst system consisting of **IC4** and **MC2**. Even at relatively high loadings of **MC2**, the rate of cross-metathesis was insufficient. More importantly, the acrylate moiety inhibited the isomerization catalyst (entries 1−4). The inhibition of double-bond migration in the presence of acrylates has been reported also for Ru−H catalyzed isomerizations concurrently or subsequently to metathesis reactions.[31]

With maleic acid (**14c**), the results were more encouraging, but the rate of cross-metathesis was still substantially lower than that of the self-metathesis of oleic acid (**1b**) (entries 5 and 6). When starting from methyl oleate (**1a**) rather than oleic acid (**1b**), the isomerizing cross-metathesis was successful, but due to the low reactivity of maleic acid, no more than one equivalent of it could be incorporated into the product mixture (entries 7 and 8). When excess maleic acid (**14c**) was used, most of it remained unchanged, thus precluding a tuning of the mean chain length by varying the stoichiometry. These results are encouraging, and it may well be possible to perform effective isomerizing cross-metatheses with this substrate combination using specially adapted metathesis catalysts.

In order to prove the concept using the catalysts systems available to us, we switched to (*E*)-3-hexenedioic acid (**14d**) as the coupling partner (entry 9). With 2 equiv of this non-conjugated dicarboxylic acid, the cross-metathesis proceeded at the same rate as the self-metathesis, and the isomerization was unaffected by the presence of the short-chain substrate (Table 4). The product distribution obtained in this cross-metathesis experiment is depicted in Figure 15. Both oleic acid (**1b**) and (*E*)-3-hexenedioic acid (**14d**) were converted

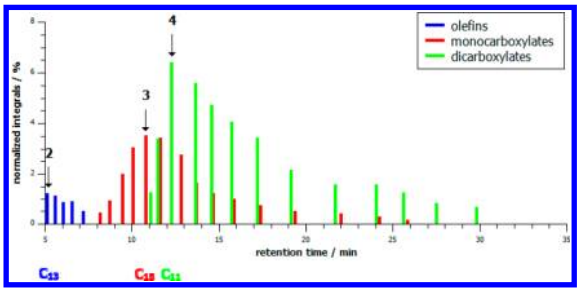

Figure 15. Product distribution of cross-metathesis of oleic acid (**1b**) with 2 equiv of (*E*)-3-hexenedioic acid (**14d**). Reaction conditions: 0.5 mmol of oleic acid (**1b**), 1.0 mmol of (*E*)-3-hexenedioic acid (**14d**), 2.5 mol % **IC4**, 5.0 mol % **MC7**, 2.0 mL THF, 60 °C, 16 h, argon atmosphere.

quantitatively. The mean chain length of all product fractions was substantially lower than in the self-metathesis of **1b**, and the dicarboxylic acid fraction became dominant.

In order to obtain a more precise picture of the relative chain-length distribution, the olefin fractions of several reactions between (*E*)-3-hexenedioic acid (**14d**) and oleic acid (**1b**) with different stoichiometries were selectively extracted and analyzed by GC and GC-MS. Figure 16 shows how the distribution maxima shift from 18 carbons for pure oleic acid (**1b**) to lower numbers. This would be expected for distributions with mean chain lengths of 10 for a 2:1 and 8 for a 5:1 ratio of (*E*)-3-hexenedioic acid (**14d**) to oleic acid (**1b**).

These studies confirm that the catalyst system remains active in the presence of (*E*)-3-hexenedioic acid (**14d**). The optimal solvent for this reaction type is THF, because it efficiently solubilizes even dicarboxylic acids.

For processes in which the low-boiling olefin fraction is continually removed by distillation to drive the equilibrium further toward the dicarboxylic acid products, this low-boiling solvent is unsuitable. We evaluated several high-boiling solvents in its place and found that Dowtherm A, a eutectic mixture of diphenyl ether and biphenyl, is also a suitable reaction solvent, although the reaction does not proceed quite as fast (Table 5).

dx.doi.org/10.1021/ja303822c | J. Am. Chem. Soc. 2012, 134, 13716−13729

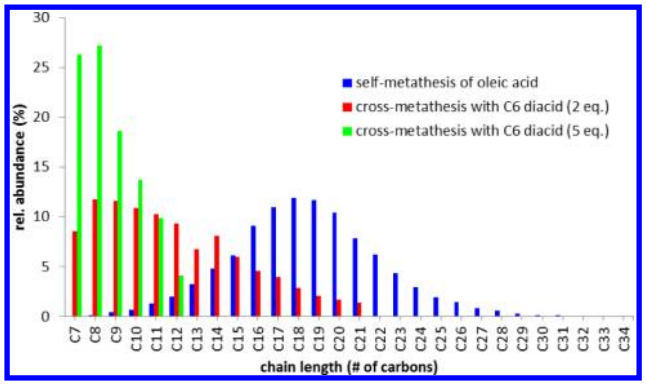

Figure 16. Chain-length distribution of the olefin fraction from isomerizing cross-metathesis of **1b** with **14d**, compared with the isomerizing self-metathesis of **1b**. Reaction conditions as given in Table 5, entry 7. Chains shorter than C_7 are unresolved due to overlapping peaks.

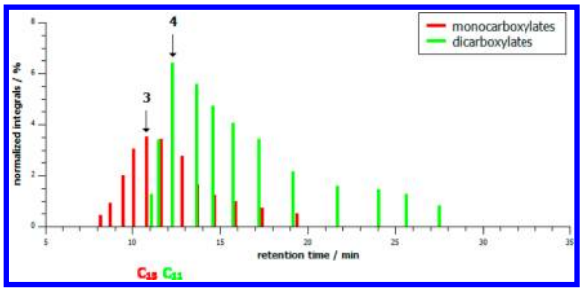

Figure 17. Product distribution of cross-metathesis of oleic acid (**1b**) with 2 equiv of (*E*)-3-hexenedioic acid (**14d**) under vacuum. Reaction conditions: 0.5 mmol of oleic acid (**1b**), 1.0 mmol of (*E*)-3-hexenedioic acid (**14d**), 2.5 mol % **IC4**, 5.0 mol % **MC7**, 60 °C, 16 h, 0.01 mbar.

Using this solvent, the olefin fraction can continuously be removed by distillation during the isomerizing metathesis. This results in a shift of the equilibrium toward the dicarboxylic acids, as illustrated by the histogram in Figure 17.

A full shift of the equilibrium toward the dicarboxylic acids should be possible using specialized equipment, such as thin-film evaporation reactors.

CONCLUSION

Our results demonstrate that isomerizing olefin metathesis is a powerful synthetic tool. Its potential applications by far surpass those of consecutive double-bond isomerization and metathesis sequences.

The discovery of the dimeric palladium(I) complex $[Pd(\mu\text{-}Br)(^tBu_3P)]_2$ as a uniquely active isomerization catalyst, which retains its activity in the presence of state-of-the-art olefin metathesis catalysts without lessening their own activity, set the stage for the development of an array of synthetic transformations involving isomerizing olefin metatheses. A particular focus was set on the utilization of long-chain unsaturated compounds derived from renewable plant-based resources.

The isomerizing self-metatheses of oleic acid and methyl oleate proceeded with impressive efficiency and turnover numbers well above 10^3. At present, metathesized fatty acid esters are tested as additives to lower the crystallization temperature of biodiesel.[32] The use of isomerizing metatheses for the same purpose would provide a broad chain-length distribution that can be expected to lead to "metathesized biodiesel" with further improved properties.

The new catalyst system is also sufficiently effective to allow conversion of mixtures of olefins with two different chain lengths into regular product distributions with mean chain lengths that can be influenced by the chain lengths of the starting materials and their ratio. The olefin blends thus obtained can be used as monomers in polymerization reactions.[33] They can also be functionalized via isomerizing hydroformylations, alkoxycarbonylations, or hydroborations, thereby providing building blocks that would otherwise only be accessible from petrochemical sources, for example, via the SHOP process.

Unsaturated dicarboxylic acids with defined chain-length distributions can be obtained via the isomerizing cross-metathesis of oleic acid with short-chain unsaturated dicarboxylic acids. Low-melting dicarboxylate mixtures are of interest, for example, for resins, coatings, or adhesives and as building blocks for polyesters and polyurethanes.[34]

In all cases, the shape of the product distributions can be influenced by the choice of the metathesis catalyst and its amount relative to that of the isomerization catalyst. A computational approach was devised that allows simulating the outcome of isomerizing self- and cross-metathesis reactions and interpreting the results obtained in the chemical reactions.

The discovery of a catalyst system with a new level of activity along with the progress made in methodically understanding isomerizing metatheses may serve as a starting point for transforming this process from a laboratory curiosity into a synthetically valuable technology.

Table 5. Optimization of the Isomerizing Cross-Metathesis of Oleic with Hexenedioic Acid[a]

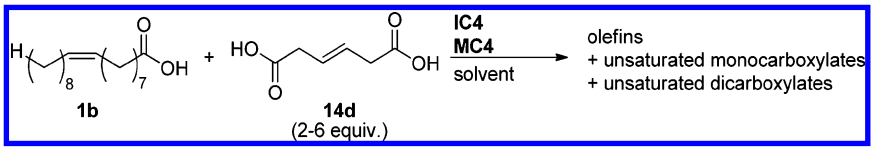

no.	**IC4** (mol %)	**MC7** (mol %)	**14d** (equiv)	solvent	conv. **1b** (%)[b]	conv. **14d** (%)
1	2.5	5.0	2	THF	98	98
2	2.5	5.0	3	THF	98	97
3	2.5	5.0	5	THF	98	97
4	2.0	3.0	2	Dowtherm A	98	85

[a]Reaction conditions: 0.50 mmol of oleic acid (**1b**), (*E*)-3-hexenedioic acid (**14d**), isomerization catalyst **IC4**, metathesis catalyst **MC7**, 2.0 mL of solvent, 60 °C, 16 h, argon atmosphere. [b]Conversion of **1b**, analysis of the product mixtures by GC after esterification with $MeOH/H_2SO_4$.

dx.doi.org/10.1021/ja303822c | J. Am. Chem. Soc. 2012, 134, 13716−13729

EXPERIMENTAL SECTION

General Methods. Reactions were performed under an argon atmosphere in oven-dried glassware containing a Teflon-coated stirrer bar and dry septum. For the exclusion of atmospheric oxygen from the reaction media, solvents were degassed and purged with argon before the reagents were mixed. Solvents were purified by standard procedures prior to use. GC analyses of isomerizing metathesis reactions of olefins were carried out using a HP-5 column, 30 m × 320 μm × 0.25 μm, split 50:1, injector temperature of 220 °C, detector temperature of 330 °C, helium carrier gas; temperature program, starting from 40 °C, hold for 5 min, heating to 250 °C at a rate of 10°/min, hold for 2 min, heating to 300 °C at a rate of 40°/min, hold for 15 min. GC analyses of isomerizing metathesis reactions of fatty acid derivatives were carried out using a HP-5 column, 30 m × 320 μm × 0.25 μm, split 50:1, injector temperature of 260 °C, detector temperature of 330 °C, helium carrier gas; temperature program, starting from 50 °C, hold for 3 min, heating to 300 °C at a rate of 8°/min, hold for 10 min. GC analyses of fatty acid isomerization studies were carried out using a crossbond PEG column, 60 m × 320 μm × 0.25 μm, split 10:1, injector temperature of 250 °C, nitrogen carrier gas; temperature program, starting from 50 °C, hold for 1 min, heating to 220 °C at a rate of 15°/min, hold for 10 min, heating to 250 °C at a rate of 15°/min, hold for 15 min. Commercial substrates were used as received unless otherwise stated. The metathesis catalysts used herein are available commercially, for example, from Sigma-Aldrich or Umicore: **MC1**, dichloro-(*o*-iso-propoxyphenylmethylene)-(tricyclohexylphosphino)ruthenium(II), CAS-no. 203714-71-0; **MC2**, 1,3-bis(mesityl)-2-imidazolidinylidene]-[2-[[(2-methylphenyl)imino]-methyl]-phenolyl]-[3-phenyl-indenyliden]-ruthenium(II)chloride, CAS-no. 934538-12-2; **MC3**, 1,3-bis(2,4,6-trimethylphenyl)-2-imidazolidinylidene]dichloro-(3-phenyl-1*H*-inden-1-ylidene)(pyridyl)-ruthenium(II), CAS-no. 1031262-76-6; **MC4**, 1,3-bis-(2,4,6-trimethyl-phenyl)-2-imidazolidinylidene)dichloro(*o*-iso-propoxyphenyl-methylene)ruthenium(II), CAS-no. 301224-40-8; **MC5**, dichloro-(3-phenyl-1*H*-inden-1-ylidene)bis(tricyclo-hexylphosphino)ruthenium(II), CAS-no. 250220-36-1; **MC6**, dichloro-(3-phenyl-1*H*-inden-1-ylidene)-bis(iso-butylphoban)ruthenium(II), CAS-no. 894423-99-5; **MC7**, 1, 3-bis(2,4,6-trimethylphenyl)-2-imidazolidinylidene-[2-[[(4-methylphenyl)imino]-methyl]-4-nitrophenolyl]-[3-phenyl-1*H*-inden-1-ylid-ene]ruthenium(II)chloride, CAS-no. 934538-04-2. The isomerization catalyst **IC4** can be obtained, for example, from Strem: dis(tri-*tert*-butylphosphino)palladiumdibromide, CAS-no. 185812-86-6.

Experimental Procedures. *Isomerization of Oleic Acid (**1b**) with Palladium Dimer **IC4** (See Table 1).* A 20 mL headspace vial with septum cap and stirring bar was charged with isomerization catalyst **IC4** (5.8 mg, 7.5 μmol). Oleic acid (**1b**) (90% purity, 942 mg, 3.0 mmol, 1.06 mL) was added via syringe, and the mixture was stirred at 70 °C for 16 h. For workup, methanol (2 mL) and 4 drops of sulfuric acid were added, and the mixture was stirred at 65 °C for 2 h. The resulting mixture was washed with aqueous bicarbonate solution (2 mL), extracted with ethyl acetate (2 mL), filtered through $MgSO_4$, and analyzed by GC. The gas chromatogram showed a distribution of double-bond isomers of methyl octadecenoates that was in good agreement with literature data on the equilibrium distribution of C_{18} methyl ester double-bond isomers. The concentration of the α,β-unsaturated isomer was determined to be 3.5%, which is an indicator that the equilibrium had been reached.[6] For full data, see Supporting Information, Figure S1.

*Self-Metathesis of Oleic Acid (**1b**) (Scheme 3).* A 20 mL headspace vial with septum cap and stirring bar was charged with metathesis catalyst **MC2** (4.2 mg, 5 μmol). Oleic acid (**1b**) (90% purity, 785 mg, 2.5 mmol, 885 μL) was added via syringe, and the mixture was stirred at 45 °C for 20 h. For workup, methanol (2 mL) and 4 drops of sulfuric acid were added, and the mixture was stirred at 65 °C for 2 h. The resulting mixture was washed with aqueous bicarbonate solution (2 mL), extracted with ethyl acetate (2 mL), filtered through $MgSO_4$, and analyzed by GC. The gas chromatogram displayed 20% methyl oleate (**1a**) corresponding to 80% conversion of **1b** into 43% of 9-octadecene (**5**) and 42% of 1,18-octadec-9-enedioic acid dimethyl ester (**6a**).

*Isomerizing Self-Metathesis of Oleic Acid (**1b**). Catalyst Screening for Table 2.* A 20 mL headspace vial with septum cap and stirring bar was charged with isomerization catalyst **IC1**−**4** (0.5 mol %) and metathesis catalyst **MC1**−**MC5** (0.2 mol %). Oleic acid (**1b**) and solvent (if appropriate) were added via syringe, and the mixture was stirred at 40−70 °C for 2−16 h. For workup, methanol (2 mL) and 4 drops of sulfuric acid were added, and the mixture was stirred at 65 °C for 2 h. The resulting mixture was washed with aqueous bicarbonate solution (2 mL), extracted with ethyl acetate (2 mL), filtered through $MgSO_4$, and analyzed by GC. The resulting distributions are provided in Figures 4 and 6−8.

Procedure To Obtain the Distribution Given in Figure 3. Following the above procedure, **1b** (90% purity, 354 mg, 1.0 mmol), catalyst **IC4** (4.9 mg, 6 μmol), catalyst **MC2** (4.2 mg, 5 μmol), and hexane (3.0 mL) were stirred for 20 h at 70 °C. The gas chromatographic signals were assigned to olefins and mono- and diesters via GC-MS and comparison to authentic samples. To generate the histograms, the relative areas for the individual compounds were plotted against their retention time, and overlapping peaks were marked with dashed lines.

Procedure To Obtain the Distribution Given in Figure 4. Following the above procedure, **1b** (90% purity, 157 mg, 0.5 mmol), catalyst **IC4** (2.1 mg, 2.5 μmol), catalyst **MC2** (2.5 mg, 3 μmol), and hexane (2.0 mL) were stirred for 2, 8, or 16 h at 60 °C. The olefins were separated as follows: NaOH solution (200 mg in methanol/water, 2.0/6.0 mL) was added to the reaction mixture. The mixture was stirred at 80 °C for 4 h to saponify the carboxylates. After cooling to 20 °C, it was extracted with hexane. The organic phase was separated, filtered through $MgSO_4$, and analyzed by GC. To generate the histograms in Figure 5, the relative areas for the individual compounds were plotted against their chain length.

Procedure To Obtain the Distribution Given in Figure 5. Following the above procedure, **1b** (90% purity, 354 mg, 1.0 mmol), catalyst **IC4** (4.9 mg, 6 μmol), catalyst **MC2** (4.2 mg, 5 μmol), and hexane (3.0 mL) were stirred for 20 h at 40 °C. The gas chromatographic signals were assigned to olefins and mono- and diesters via GC-MS and comparison to authentic samples. To generate the histograms, the relative areas for the individual compounds were plotted against their retention time, and overlapping peaks were marked with dashed lines.

Procedure to Obtain the Distribution Given in Figure 6. Following the above procedure, **1b** (90% purity, 354 mg, 1.0 mmol), catalyst **IC4** (4.9 mg, 6 μmol), and catalyst **MC2** (4.2 mg, 5 μmol) were stirred for 8 h at 60 °C. The gas chromatographic signals were assigned to olefins and mono- and diesters via GC-MS and comparison to authentic samples. To generate the histograms, the relative areas for the individual compounds were plotted against their retention time, and overlapping peaks were marked with dashed lines.

Procedure To Obtain the Distribution Given in Figure 7. Following the above procedure, **1b** (90% purity, 354 mg, 1.0 mmol), catalyst **IC4** (2.5 mg, 3 μmol), catalyst **MC3** (3.7 mg, 5 μmol), and hexane (3.0 mL) were stirred for 20 h at 50 °C. The gas chromatographic signals were assigned to olefins and mono- and diesters via GC-MS and comparison to authentic samples. To generate the histograms, the relative areas for the individual compounds were plotted against their retention time, and overlapping peaks were marked with dashed lines.

Isomerizing Self-Metathesis of 10-Undecenoic Acid (7) (Scheme 4). A 20 mL headspace vial with septum cap and stirring bar was charged with isomerization catalyst **IC4** (3.9 mg, 2.5 μmol) and metathesis catalyst **MC2** (2.5 mg, 3 μmol). 10-Undecenoic acid (7) (98% purity, 94 mg, 0.5 mmol) and hexane (3 mL) were added via syringe, and the mixture was stirred at 70 °C for 20 h. For workup, methanol (2 mL) and 4 drops of sulfuric acid were added, and the mixture was stirred at 65 °C for 2 h. The resulting mixture was washed with aqueous bicarbonate solution (2 mL), extracted with ethyl acetate (2 mL), filtered through $MgSO_4$, and analyzed by GC and GC-MS. The gas chromatograms showed a mixture of C_{11}−C_{16} olefins, C_7−C_{24} unsaturated monoesters, and C_{11}−C_{24} unsaturated diesters.

dx.doi.org/10.1021/ja303822c | J. Am. Chem. Soc. 2012, 134, 13716−13729

Isomerizing Self-Metathesis of Linoleic Acid (8) (Scheme 4). In an analogous procedure, linoleic acid (90% purity, 140 mg, 0.5 mmol) was converted into a mixture of C_{11}−C_{22} diolefins, C_9−C_{24} diunsaturated monoesters, and C_8−C_{22} diunsaturated diesters.

Isomerizing Self-Metathesis of (*E*)-3-Hexene (9) (Figure 8, Red Bars). A 20 mL headspace vial with septum cap and stirring bar was charged with isomerization catalyst **IC4** (4.1 mg, 5.0 μmol) and metathesis catalyst **MC4** (3.8 mg, 6.0 μmol). (*E*)-3-Hexene (**9**) (86 mg, 127 μL, 1.00 mmol) and toluene (1.0 mL) were added via syringe, and the mixture was stirred at 45 °C for 16 h. After cooling to 20 °C, the mixture was diluted with toluene (3 mL), filtered through a basic alumina plug and analyzed by GC and GC-MS. The gas chromatogram of the mixture displayed olefins with the chain-length distribution provided in the Supporting Information, Table S2.

Sequential Isomerization and Self-Metathesis of (*E*)-3-Hexene (9) (Figure 8, Blue Bars). A 20 mL headspace vial with septum cap and stirring bar was charged with isomerization catalyst **IC4** (10 mg, 12.5 μmol). Via syringe, toluene (1.0 mL) and (*E*)-3-hexene (**9**) (43 mg, 63 μL, 0.50 mmol) were added, and the mixture was stirred at 45 °C for 16 h. After cooling to 20 °C, the mixture was filtered through a basic alumina plug into another reaction vial to remove the palladium catalyst. A solution of metathesis catalyst **MC4** (7.72 mg, 12.3 μmol) in degassed toluene (0.5 mL) was added, and the mixture was stirred for 16 h at 45 °C. After cooling to 20 °C, the mixture was diluted with toluene (3 mL), filtered through a basic alumina plug, and analyzed by GC. The gas chromatogram of the mixture showed olefins with the chain-length distribution provided in the Supporting Information, Table S3.

Sequential Isomerization and Cross-Metathesis of (*E*)-3-Hexene (9) and 1-Octadecene (11) (Figure 9, Red Bars). A 20 mL headspace vial with septum cap and stirring bar was charged with isomerization catalyst **IC4** (10 mg, 12.5 μmol). Via syringe, toluene (1.0 mL), (*E*)-3-hexene (**9**) (43 mg, 63 μL, 0.50 mmol), and 1-octadecene (**11**) (66 mg, 84 μL, 0.25 mmol) were added, and the mixture was stirred at 45 °C for 16 h. After cooling to 20 °C, the mixture was filtered through a basic alumina plug into another reaction vial to remove the palladium catalyst. A solution of metathesis catalyst **MC4** (7.72 mg, 12.3 μmol) in degassed toluene (0.5 mL) was added, and the mixture was stirred for 16 h at 45 °C. After cooling to 20 °C, the mixture was diluted with toluene (3 mL), filtered through a basic alumina plug, and analyzed by GC. The gas chromatogram of the mixture showed olefins with the chain-length distribution provided in the Supporting Information, Table S5.

Isomerizing Cross-Metathesis of (*E*)-3-Hexene (9) with 1-Octadecene (11) Leading to the Dishtributions Given in Figure 10. A 20 mL headspace vial with septum cap and stirring bar was charged with isomerization catalyst **IC4** (4.1 mg, 5 μmol) and metathesis catalyst **MC4** (3.8 mg, 6 μmol). (*E*)-3-Hexene (**9**) (43 mg, 63 μL, 0.5 mmol), 1-octadecene (**11**) (0.5−2 equiv), and toluene (1.0 mL) were added via syringe, and the mixture was stirred at 45 °C for 16 h. The gas chromatogram of the reaction mixture showed olefins with the chain-length distribution displayed in Figure 10. For the reaction in the presence of 0.5 equiv of **11** (66.4 mg, 84 μL, 0.25 mmol), the chain-length distribution is provided in the Supporting Information, Table S4.

Isomerizing Ethenolysis of Oleic Acid (1b) (Figure 14). A 20 mL headspace vial with septum cap and stirring bar was charged with isomerization catalyst **IC4** (3.1 mg, 3.8 μmol) and metathesis catalyst **MC7** (6.7 mg, 7.5 μmol), and purged three times with ethylene (purity N30, atmospheric pressure). Oleic acid (**1b**) (99%, 143 mg, 161 μL, 0.50 mmol) and hexane (3.0 mL) were added via syringe, and the mixture was stirred at 50 °C for 16 h. In order to analyze the olefin fraction in detail, separation of the olefins was accomplished as follows: To the reaction mixture was added NaOH solution (200 mg in methanol/water, 2.0/6.0 mL). The mixture was stirred at 80 °C for 4 h, and after cooling to 20 °C, it was extracted with hexane. The organic phase was separated, filtered through $MgSO_4$, and analyzed by GC. The olefin fraction displayed the chain-length distribution provided in the Supporting Information, Table S6.

Isomerizing Cross-Metathesis of Oleic Acid (1b) and (*E*)-3-Hexenedioic Acid (14d) (Figure 16). A 20 mL headspace vial with septum cap and stirring bar was charged with isomerization catalyst **IC4** (5.1 mg, 6.3 μmol), metathesis catalyst **MC7** (7.9 mg, 12.5 μmol), and (*E*)-3-hexenedioic acid **14d** (74 mg, 0.5 mmol, 2.0 equiv.). Oleic acid (**1b**) (99% purity, 71 mg, 80 μL, 0.25 mmol) and THF (1.0 mL) were added via syringe, and the mixture was stirred at 60 °C for 16 h. The olefins were separated as follows: NaOH solution (200 mg in methanol/water, 2.0/6.0 mL) was added to the reaction mixture. The mixture was stirred at 80 °C for 4 h to saponify the carboxylates. After cooling to 20 °C, it was extracted with hexane. The organic phase was separated, filtered through $MgSO_4$, and analyzed by GC and GC-MS. The olefin fraction displayed the chain-length distribution provided in the Supporting Information, Table S7.

Simulations of Olefin Product Distributions. All computations were carried out using the R statistics software.[30] The input text for all simulations is detailed in the Supporting Information. The output was generated in the form of .txt files that were then imported into MS Excel for generation of histograms.

■ ASSOCIATED CONTENT

Ⓢ Supporting Information

Gas chromatographic data and the simulation program code. This material is available free of charge via the Internet at http://pubs.acs.org.

■ AUTHOR INFORMATION

Corresponding Author

goossen@chemie.uni-kl.de

Notes

The authors declare no competing financial interest.

■ ACKNOWLEDGMENTS

We thank NanoKat, the Collaborative Research Centre SFB/TRR 88 "3MET", the Stiftung der Deutschen Wirtschaft (fellowship to D.M.O.), and the Carl Zeiss Foundation (Center for Mathematical and Computational Modeling (CM)^2 fellowship to N.T.) for financial support, and Umicore AG for the donation of chemicals.

■ REFERENCES

(1) Arpe, H.-J. *Industrielle organische Chemie: bedeutende Vor- und Zwischenprodukte*, 6th ed.; Wiley-VCH: Weinheim, Germany, 2007, pp 94−95.

(2) Biermann, U.; Bornscheuer, U.; Meier, M. A. R.; Metzger, J. O.; Schäfer, H. J. *Angew. Chem.* **2011**, *123*, 3938−3956; *Angew. Chem., Int. Ed.* **2011**, *50*, 3854−3871.

(3) (a) Carlsson, A. S.; Lindberg Yilmaz, J.; Green, A. G.; Stymne, S.; Hofvander, P. *Eur. J. Lipid Sci. Technol.* **2011**, *113*, 812−831. (b) Hill, K. *Pure Appl. Chem.* **2007**, *79*, 1999−2011. (c) Ronda, J. C.; Lligadas, G.; Galià, M.; Cádiz, V. *Eur. J. Lipid Sci. Technol.* **2011**, *113*, 46−58. (d) Meier, M. A. R.; Metzger, J. O.; Schubert, U. S. *Chem. Soc. Rev.* **2007**, *36*, 1788−1802. (e) Xia, Y.; Larock, R. C. *Green Chem.* **2010**, *12*, 1893−1909.

(4) Behr, A.; Obst, D.; Westfechtel, A. *Eur. J. Lipid Sci. Technol.* **2005**, *107*, 213−219.

(5) (a) Jiménez-Rodriguez, C.; Eastham, G. R.; Cole-Hamilton, D. J. *Inorg. Chem. Commun.* **2005**, *8*, 878−881. (b) Jiménez-Rodriguez, C.; Eastham, G. R.; Cole-Hamilton, D. J. *Chem. Commun.* **2004**, 1720−1721. (c) Quinzler, D.; Mecking, S. *Angew. Chem.* **2010**, *122*, 4402−4404;(d) *Angew. Chem., Int. Ed.* **2010**, *49*, 4306−4308.

(6) Ghebreyessus, K. Y.; Angelici, R. J. *Organometallics* **2006**, *25*, 3040−3044.

(7) (a) Gooßen, L. J.; Ohlmann, D. M.; Dierker, M. *Green Chem.* **2010**, *12*, 197−200. (b) Gooßen, L. J.; Ohlmann, D. M.; Dierker, M.; Löhl, T. European Patent EP 22411562, 2009.

(8) (a) Ohlmann, D. M.; Gooßen, L. J.; Dierker, M. *Chem.—Eur. J.* **2011**, *17*, 9508−3519. (b) Gooßen, L. J.; Ohlmann, D. M.; Dierker, M. European Patent EP 10189314, 2010.
(9) Porri, L.; Diversi., P.; Lucherini, A.; Rossi, R. *Makromol. Chem.* **1975**, *176*, 3121−3125.
(10) France, M. B.; Feldman, J.; Grubbs, R. H. *J. Chem. Soc., Chem. Commun.* **1994**, 1307−1308.
(11) Consorti, C. S.; Aydos, G. L. P.; Dupont, J. *Chem. Commun.* **2010**, *46*, 9058−9060.
(12) (a) Johnson, R. W. *Fatty Acids in Industry: Processes, Properties, Derivatives, Applications*. Marcel Dekker Inc.: New York, 1989. (b) Huf, S.; Krügener, S.; Hirth, T.; Rupp, S.; Zibek, S. *Eur. J. Lipid Sci. Technol.* **2011**, *113*, 548−561. (c) Schindler, J.; Meussdoerffer, F.; Giesel-Buehler, H. *Forum Mikrobiol.* **1990**, *13*, 274−281. (d) Pic-ataggio, S.; Rohrer, T.; Deanda, K.; Lanning, D.; Reynolds, R.; Mielenz, J.; Eirich, L. D. *Nat. Biotechnol.* **1992**, *10*, 894−898.
(13) (a) Schmidt, B. *Eur. J. Org. Chem.* **2003**, 816−819. (b) Schmidt, B. *J. Org. Chem.* **2004**, *69*, 7672−7687. (c) Gauthier, D.; Lindhardt, A. T.; Olsen, E. P. K.; Overgaard, J.; Skrydstrup, T. *J. Am. Chem. Soc.* **2010**, *132*, 7998−8009.
(14) (a) Barton, D. H. R.; Davies, S. G.; Motherwell, W. B. *Synthesis* **1979**, 265−266. (b) Wakamatsu, H.; Nishida, M.; Adachi, N.; Mori, M. *J. Org. Chem.* **2000**, *65*, 3966−3970. (c) Singer, H.; Stein, W.; Lepper, H. *Fette, Seifen, Anstrichm.* **1972**, *74*, 193−198. (d) Salvini, S.; Piacenti, F.; Frediani., P.; Devescovi, A.; Caporali, M. *J. Organomet. Chem.* **2001**, *625*, 255−267. (e) Laï, R.; Ucciani, E.; Naudet, M. *Bull. Soc. Chim. Fr.* **1969**, *3*, 793−797. (f) Rhoads, S. J.; Chattopadhyay, J. K.; Waali, E. E. *J. Org. Chem.* **1970**, *35*, 3352−3358.
(15) For the synthesis and properties of **IC4**, see: (a) Vilar, R.; Mingos, D. M. P.; Cardin, C. J. *J. Chem. Soc., Dalton Trans.* **1996**, *23*, 4313−4314. (b) Colacot, T. J. *Platinum Metals Rev.* **2009**, *53*, 183−188. (c) Durá-Vilá, V.; Mingos, D. M. P.; Vilar, R.; White, A. J. P.; Williams, D. J. *J. Organomet. Chem.* **2000**, *600*, 198−205. (d) Colacot, T. J.; Hooper, M. W.; Grasa, G. A. International Patent WO 2011/012889A1, 2011. (e) Gooßen, L. J.; Mamone, P.; Grünberg, M. F.; Arndt, M. European Patent EP 11005326, 2011.
(16) For examples of C−C couplings, see: (a) Huang, J.; Bunel, E.; Faul, M. M. *Org. Lett.* **2007**, *9*, 4343−4346. (b) Stambuli, J. P.; Kuwano, R.; Hartwig, J. F. *Angew. Chem., Int. Ed.* **2002**, *41*, 4746−4748. (c) Hama, T.; Liu, X.; Culkin, D. A.; Hartwig, J. F. *J. Am. Chem. Soc.* **2003**, *125*, 11176−11177. (d) Hama, T.; Hartwig, J. F. *Org. Lett.* **2008**, *10*, 1545−1548. (e) Hama, T.; Hartwig, J. F. *Org. Lett.* **2008**, *10*, 1549−1552. For examples of C−N and C−S couplings, see: (f) Ryberg, P. *Org. Process Res. Dev.* **2008**, *12*, 540−543. (g) Prashad, M.; Mak, X. Y.; Liu, Y.; Repic, O. *J. Org. Chem.* **2003**, *68*, 11C63−1164. (h) Eichmann, C. C.; Stambuli, J. P. *J. Org. Chem.* **2009**, *74*, 4005−4008. For recently developed C−Si couplings, see: (i) Hemgesberg, M.; Ohlmann, D. M.; Schmitt, Y.; Wolfe, M.; Müller, M. K.; Erb, B.; Sun, Y.; Gooßen, L. J.; Gerhards, M.; Thiel, W. R. *Eur. J. Org. Chem.* **2012**, *11*, 2142−2151.
(17) For reviews on double-bond migration of olefins, see: (a) Smith, M. B.; March, J. *March's Advanced Organic Chemistry*, 6th Ed.; John Wiley & Sons, Inc.: Hoboken, NJ, 2007; pp 767−772, and references therein. (b) Rodriguez, J.; Brun, P.; Waegell, B. *Bull. Soc. Chim. Fr.* **1989**, 799−823. (c) Jardine, F. R. In *The Chemistry of the Metal-Carbon Bond*; Hartley, F. R., Patai, S., Eds.; Wiley: New York, 1987; Vol. *4*, pp 733−818. (d) Schunn, R. A. *Inorg. Chem.* **1970**, *9*, 2567−2572.
(18) (a) Cermak, S. C.; Isbell, T. A. *J. Am. Oil Chem. Soc.* **2001**, *78*, 557−565. (b) Isbell, T. A.; Frykman, H. B.; Abbott, T. P.; Lohr, J. E.; Drozd, J. C. *J. Am. Oil Chem. Soc.* **1997**, *74*, 473−477.
(19) Yoshida, T.; Otsuka, S. *J. Am. Chem. Soc.* **1977**, *99*, 2134−2140.
(20) Barrios-Landeros, F.; Carrow, B. P.; Hartwig, J. F. *J. Am. Chem. Soc.* **2008**, *130*, 5842−5843.
(21) Mamone, P.; Grünberg, M. F.; Fromm, A.; Khan, B. A.; Gooßen, L. J. *Org. Lett.* **2012**, *14*, 3716−3719.
(22) (a) Harrity, J. P. A.; La, D. S.; Cefalo, D. R.; Visser, M. S.; Hoveyda, A. H. *J. Am. Chem. Soc.* **1998**, *120*, 2343−2351. (b) Kingsbury, J. S.; Harrity, J. P. A.; Bonitatebus, P. J.; Hoveyda, A. H. *J. Am. Chem. Soc.* **1999**, *121*, 791−799.
(23) Verpoort, F. W. C.; De Clercq, B. International Patent WO2003062253, 2003.
(24) (a) Clavier, H.; Nolan, S. P. *Chem.—Eur. J.* **2007**, *13*, 8029−8036. (b) Monsaert, S.; Drozdzak, R.; Dragutan, V.; Dragutan, I.; Verpoort, F. *Eur. J. Inorg. Chem.* **2008**, 432−440.
(25) (a) Garber, S. B.; Kingsbury, J. S.; Gray, B. L.; Hoveyda, A. H. *J. Am. Chem. Soc.* **2000**, *122*, 8168−8179. (b) Gessler, S.; Randl, S.; Blechert, S. *Tetrahedron Lett.* **2000**, *41*, 9973−9976.
(26) (a) Fürstner, A.; Guth, O.; Düffels, A.; Seidel, G.; Liebl, M.; Gabor, B.; Mynott, R. *Chem.—Eur. J.* **2001**, *7*, 4811−4820. (b) Mierde, H. V.; Van Der Voort, P.; De Vos, D.; Verpoort, F. *Eur. J. Org. Chem.* **2008**, 1625−1631. (c) Boeda, F.; Clavier, H.; Nolan, S. P. *Chem. Commun.* **2008**, 2726−2740.
(27) Sasol Technology UK and Umicore AG and Co KG. International Patent WO 2007/010453 A2, 2007.
(28) (a) Ngo, H. L.; Jones, K.; Foglia, T. A. *J. Am. Oil Chem. Soc.* **2006**, *83*, 629−634. (b) Samorski, M.; Dierker, M. European Patent EP 2157076, 2008.
(29) For the reaction of 1,3-dienes with iron carbonyl, see: (a) Knölker, H.-J. *Chem. Soc. Rev.* **1999**, *28*, 151−157. For coordination modes of 1,3-dienes, see: (b) Mashima, K.; Nakamura, A. *J. Organomet. Chem.* **2002**, *663*, 5−12. For the synthesis of conjugated plant oils, see: (c) Quirino, R. L.; Larock, R. C. *J. Am. Oil Chem. Soc.* **2012**, *89*, 1113−1124.
(30) R Development Core Team *R: A language and environment for statistical computing*; R Foundation for Statistical Computing, Vienna, Austria, 2010. ISBN 3-900051-07-0, URL http://www.R-project.org/.
(31) (a) Djigoué, G. B.; Meier, M. A. R. *Appl. Catal., A* **2009**, *368*, 158−162. (b) Schmidt, B.; Geißler, D. *ChemCatChem* **2010**, *2*, 423−429.
(32) (a) Marvey, B. B. *Int. J. Mol. Sci* **2008**, *9*, 1393−1406. (b) Montenegro, R. E.; Meier, M. A. R. *Eur. J. Lipid Sci. Technol.* **2012**, *114*, 55−62.
(33) Heublein, G.; Hartung, H.; Helbig, M.; Stadermann, D. *J. Macromol. Sci., Chem.* **1982**, *17*, 821−845.
(34) (a) Johnson, R. W. *Fatty Acids in Industry: Processes, Properties, Derivatives, Applications*. Marcel Dekker Inc.: New York, 1989. (b) Huf, S.; Krügener, S.; Hirth, T.; Rupp, S.; Zibek, S. *Eur. J. Lipid Sci. Technol.* **2011**, *113*, 548−561. (c) Schindler, J.; Meussdoerffer, F.; Giesel-Buehler, H. *Forum Mikrobiol.* **1990**, *13*, 274−281. (d) Pic-ataggio, S.; Rohrer, T.; Deanda, K.; Lanning, D.; Reynolds, R.; Mielenz, J.; Eirich, L. D. *Nat. Biotechnol.* **1992**, *10*, 894−898.

NOTE ADDED AFTER ASAP PUBLICATION

This paper was published ASAP on August 9, 2012. The captions to Tables 4 and 5 have been updated. The revised version was posted on August 13, 2012.